Polymerization of Bis(triethoxysilyl)ethenes. Impact of Substitution Geometry on the Formation of Ethenylene- and Vinylidene-Bridged Polysilsesquioxanes

Douglas A. Loy,*,† Joseph P. Carpenter,† Stacey A. Yamanaka,† Mark D. McClain,† John Greaves,‡ Steven Hobson,‡ and Kenneth J. Shea*,‡

Encapsulants and Foams Department, Sandia National Laboratories, Albuquerque, New Mexico 87185-1407, and Department of Chemistry, University of California at Irvine, Irvine, California 92717

Received August 1, 1998. Revised Manuscript Received August 18, 1998

In this study, we utilized the substitution geometry of triethoxysilyl groups about an organic bridging group to control the outcome of the sol−gel polymerization process. The substitution geometry of two triethoxysilyl groups about a carbon−carbon double bond was determined to have a profound effect on sol−gel polymerizations of the *E* (**1**) and *Z* (**2**) ethenylene-bridged monomers and vinylidene-bridged monomer (**3**) and on the porosity in the resulting xerogels. ^{29}Si NMR and chemical ionization mass spectrometry were used to elucidate the early sol−gel chemistry in the acid-catalyzed polymerizations of **1**−**3**. Trans substitution about the ethenylene-bridging group in **1** led to acyclic and monocyclic dimers and trimers as condensation products under acidic conditions and only microporous gels under both acidic and basic conditions. In contrast, cyclization reactions dominated the sol−gel chemistry of **2** beginning with intramolecular cyclization to give the cyclic disilsesquioxane (**4**) and continued with the formation of cyclic oligomers, including a bicyclic dimer. The cyclization of **2** slowed the rate of gelation compared to **1** and afforded microporous xerogels under acidic conditions and mesoporous gels under basic conditions. The sol−gel chemistry of the vinylidene monomer (**3**) was strongly retarded by the formation of a cyclic dimer (**5**). Only mesoporous gels were formed under basic conditions after 9 months; no gels were obtained under acidic conditions.

Introduction

An objective of contemporary materials chemistry is to develop insight into the relationship between molecular building blocks or low molecular weight precursors and the bulk properties of the resultant material. These objectives can be approached to some degree with simple linear organic polymers. More complex substances such as network polymers and inorganic oxides present far greater challenges. Sol−gel chemistry falls into this latter category.[1] The polyfunctionality of the starting monomers, the sensitivity of key reactions to the nature of the catalyst, the competition between kinetic and thermodynamic driven processes, phase separation, and physical and chemical processes that accompany subsequent processing of the material are only a partial list of factors that contribute to the morphology of the final xerogel. Despite these intimidating obstacles the technological importance of these materials justifies efforts to this end. Bridged polysilsesquioxanes, a family of sol−gel-derived hybrid materials, provide a unique arena for such an investigation (Scheme 1).[2] The molecular building blocks used for their synthesis are comprised of a variable organic component and an inorganic oxide precursor. Prior studies note that small changes in the variable organic component result in profound changes in the final properties (surface area, pore size, and thermal stability) of the resulting xerogel.[2]

Scheme 1

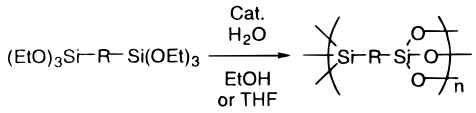

Cat. = ^+H or ^-OH

R = alkylene or arylene.

For example, rigid arylene-bridging groups have been shown to give rise to materials with high surface areas with a relatively large contribution from micropores (<20 Å).[3] The length of alkylene-bridging groups can be used to control the size and dispersity of pores in hydrocarbon-bridged xerogels.[4] Collapse of pores during drying to give nonporous[5] materials was observed to be dependent on both length of the alkylene bridge and the

† Sandia National Laboratories. E-mail: daloy@sandia.gov.
‡ University of California.

(1) Brinker, C. J.; Scherer, G. W. *Sol−Gel Science: the physics and chemistry of sol−gel processing,* 1st ed.; Academic Press: San Diego, CA, 1990.
(2) Loy, D. A.; Shea, K. J. *Chem. Rev.* **1995**, *95*, 1431−42.
(3) Shea, K. J.; Loy, D. A.; Webster, O. *J. Am. Chem. Soc.* **1992**, *114*, 6700−10.
(4) Oviatt, H. W., Jr.; Shea, K. J.; Small, J. H. *Chem. Mater.* **1993**, *5*, 943−50.
(5) Nonporous to nitrogen sorption porosimetry.

10.1021/cm9805424 CCC: $15.00
Published on Web 11/10/1998

degree of condensation at the silsesquioxane groups. Only alkylene bridges of four carbons or less give rise to porous materials independent of the degree of condensation. These results suggest that rigidity in the organic bridge may be essential to maintain porosity and a high surface area in polysilsesquioxanes.[6]

Introduction of olefinic functionalitites into alkylene-bridging groups not only provides the opportunity to reduce the conformational freedom of the bridging group but also provides a convenient π-ligand site for attaching metals into a polysilsesquioxane network polymer.[7] In this study, we have examined the preparation of ethenylene-bridged polysilsesquioxanes from the *E*-(**1**) and

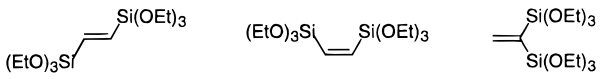

1 **2** **3**

Z-(**2**) isomers of 1,2-bis(triethoxysilyl)ethene and vinylidene-bridged polysilsesquioxanes from 1,1-bis(triethoxysilyl)ethene (**3**). The absence of flexible methylenes (CH_2) results in short, rigid bridging groups which are expected to yield porous materials. This study was also intended to determine the effects of the substitution geometry about the carbon−carbon double bond on the condensation chemistry of the monomers and on the resulting architectures of the final materials. For example, the *Z*-isomer has the potential to form the monomeric disilaoxacyclopentene **4** through an intramolecular condensation reaction.[8] This phenomenon has been observed with ethylene-, propylene-, and butylene-bridged systems which exhibited prolonged gel times under acidic conditions due to intramolecular cyclizations of the monomers.[9] Intramolecular condensation of **1** would be precluded by the *E* substitution geometry about the bridging olefin. The structure of the initial condensation products could play a significant role in the polymerization rate and in the structure of the ethenylene-bridged polysilsesquioxanes.

The early hydrolysis and condensation chemistry of **1**−**3** was examined under acidic conditions by solution ^{29}Si NMR spectroscopy and chemical ionization mass spectrometry. Each monomer was found to have its own unique condensation process as outlined in Scheme 2. While the *E* and *Z* isomers polymerize through acyclic and cyclic condensations, **3** forms a cyclic dimer (**5**) that is resistant toward further condensation reactions. The effects of these structures on the final architectures of the ethenylene-bridged polysilsesquioxane xerogels were determined by solid-state ^{13}C and ^{29}Si CP MAS (cross polarization magic angle spinning) NMR spectroscopy, scanning electron microscopy, and nitrogen sorption porosimetry. Significant differences in the gelation of the three monomers and in the properties of the final

Scheme 2

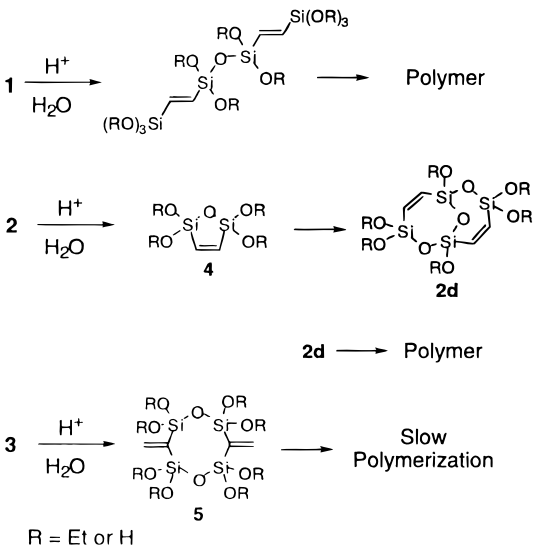

xerogels are related to the early sol−gel chemistry observed during the polymerization of each monomer.

Experimental Section

General Methods. Ethanol was distilled from magnesium before use. Anhydrous THF, triethoxyvinylsilane, and $RuCl_2(PPh_3)_3$ were used as received from Aldrich. ^{1}H nuclear magnetic resonance (NMR) spectra were recorded on a Bruker AM300 (300 MHz) using C_6D_6 as the solvent. Infrared spectra were obtained using a Perkin-Elmer 1750 FTIR spectrophotometer. The spinning band apparatus was from BR Instrument Corp. Mass spectra were obtained on a Fisons Autospec (CI, ammonia). Monomer purity was determined by GC with an HP Series II 5890 and a packed column with HP-1 (cross-linked methyl siloxane), 15 m × 0.32 mm.

Monomer Preparation. *(E)-1,2-Bis(triethoxysilyl)ethene (**1**) and 1,1-Bis(triethoxysilyl)ethene (**3**).* A mixture of **1** (84%) and **3** (16%) was prepared by the reaction of triethoxyvinylsilane (125 mL, 0.593 mol) with $RuCl_2(PPh_3)_3$ (0.304 g, 0.317 mmol) at reflux for 24 h.[10,11] Residual triethoxyvinylsilane was distilled off at atmospheric pressure, and the remaining liquid was purified by spinning band vacuum distillations (2×). Monomer **1** (62.6 g, 98% by GC, yield = 60%) was collected as a clear, colorless oil at 90 °C/15 μm): IR (film on NaCl) 2975, 2928, 2886, 2736, 1442, 1391, 1295, 1168, 1104, 1021, 961, 784 cm^{-1}; ^{1}H NMR (300 MHz, C_6D_6) δ 7.05 (s, 2 H, C*H*Si(OEt)$_3$), 3.83 (q, 12 H, J = 7.0 Hz, OC*H*$_2$CH$_3$), 1.16 (t, 18 H, J = 7.0 Hz, OCH$_2$C*H*$_3$); ^{13}C NMR (75.5 MHz, C_6D_6) δ 146.34 (*C*HSi(OEt)$_3$), 58.79 (O*C*H$_2$CH$_3$), 18.48 (OCH$_2$*C*H$_3$); ^{29}Si NMR (79.5 MHz, ethanol) δ −61.13; low-resolution mass spectrum (CI, ammonia) m/z 370 [M + NH$_4$]$^+$, 353 [M + H]$^+$; high-resolution mass spectrometry (CI, ammonia) m/z calcd for $C_{14}H_{32}O_6Si_2$ + H 353.1815, found 353.1812. Monomer **3** (6.3 g, 99% by GC, yield = 6%) was collected as a clear, colorless oil at 65 °C/15 μm: IR (film on NaCl) 2975, 2928, 2886, 2736, 1571, 1483, 1443, 1418, 1391, 1296, 1168, 1104, 1083, 962, 860, 787 cm^{-1}; ^{1}H NMR (300 MHz, C_6D_6) δ 6.96 (s, 2 H, C*H*$_2$), 3.92 (q, 12 H, J = 7.0 Hz, OC*H*$_2$CH$_3$), 1.16 (t, 18 H, J = 7.0 Hz, OCH$_2$C*H*$_3$); ^{13}C NMR (75.5 MHz, C_6D_6) δ 150.46 (*C*H$_2$), 139.54 {*C*[Si(OEt)$_3$]$_2$}, 58.73 (O*C*H$_2$CH$_3$), 18.47 (OCH$_2$*C*H$_3$); ^{29}Si NMR (79.5 MHz, CD_3CD_2OD) δ −58.02; low-resolution mass spectrum (CI, ammonia) m/z 370 [M + NH$_4$]$^+$, 353 [M + H]$^+$; high-resolution mass spectrometry (CI, ammonia) m/z calcd for $C_{14}H_{32}O_6Si_2$ + H 353.1815, found 353.1812.

(6) Differences in hydrophobicity due to alkylene-bridging group length and degree of condensation may also contribute to the collapse of the porosity by modifying the solvent−gel interactions during drying.

(7) Corriu, R. J. P.; Moreau, J. J. E.; Thepot, P.; Man, M. W. C. *J. Mater. Chem* **1994**, *4*, 987−9.

(8) Disilaoxacyclopentanes have been prepared from the hydrolysis and condensation of bis(chlorodimethylsilyl)ethane: Seyferth, D.; Robison, J. *Macromolecules* **1993**, *26*, 407−18.

(9) Loy, D. A.; Carpenter, J. P.; Myers, S. A.; Assink, R. A.; Small, J. H.; Greaves, J.; Shea, K. J. *J. Am. Chem. Soc.* **1996**, *118*, 8501−8502.

(10) Marciniec, B.; Maciejewski, H.; Gulindki, J.; Rzejak, J. *J. Organomet. Chem.* **1989**, *362*, 273.

(11) Marciniec, B.; Pietraszuk, C. *J. Chem. Soc., Chem. Commun.* **1995**, 2003.

(*Z*)-*1,2-Bis(triethoxysilyl)ethene (**2**).* A photolysis tube was charged with (*E*)-1,2-bis(triethoxysilyl)ethene (280 g, 0.795 mol) and benzophenone (100 mg, 0.549 mmol). Irradiation for 25 h with a 1000 W mercury lamp, under an argon atmosphere, yielded a mixture of the *E* (71%) and Z (25%) isomers. Spinning band vacuum distillation (2×) of the mixture afforded 26.6 g (10%) of (*Z*)-1,2-bis(triethoxysilyl)ethene (>96% by GC) as a colorless oil: bp 65−70 °C/20 μm: IR (film on NaCl) 2975, 2928, 2886, 2736, 1443, 1391, 1351, 1295, 1168, 1104, 1083, 961, 789, 755 cm^{-1}; ^{1}H NMR (300 MHz, C_6D_6) δ 6.74 (s, 2 H, C*H*Si(OEt)$_3$), 3.86 (q, 12 H, J = 7.0 Hz, OC*H*$_2$CH$_3$), 1.22 (t, 18 H, J = 7.0 Hz, OCH$_2$C*H*$_3$); ^{13}C NMR (75.5 MHz, C_6D_6) δ 146.29 (*C*HSi(OEt)$_3$), 58.60 (O*C*H$_2$CH$_3$), 18.45 (OCH$_2$*C*H$_3$); ^{29}Si NMR (79.5 MHz, ethanol) δ −61.91; low-resolution mass spectrum (CI, ammonia) *m*/*z* 370 [M + NH$_4$]$^+$, 353 [M + H]$^+$; high-resolution mass spectrometry (CI, ammonia) *m*/*z* calcd for $C_{14}H_{32}O_6Si_2$ + H 353.1815, found 353.1820.

Isolation of Cyclic Condensation Products. *Cyclic Disilsesquioxane (**4**).* A flask was charged with (*Z*)-1,2-bis(triethoxysilyl)ethene (12.4 g, 35 mmol), aqueous HCl (0.63 mL, 1 N, 35 mmol H_2O), and THF (85 mL). After stirring of the mixture for 48 h, conversion to the cyclic product was 90% by GC. The solvent was removed in vacuo, and the crude oil was vacuum distilled yielding 6.5 g (67%) of **4** (96% by GC): bp 50−51 °C/70 μm; IR (film on NaCl) 2977, 2929, 2891, 2736, 1444, 1392, 1309, 1170, 1104, 1083, 955, 830, 794, 713 cm^{-1}; ^{1}H NMR (300 MHz, C_6D_6) δ 6.89 (s, 2 H, C*H*Si(OEt)$_3$), 3.79 (q, 8 H, J = 7.0 Hz, OC*H*$_2$CH$_3$), 1.11 (t, 12 H, J = 7.0 Hz, OCH$_2$-C*H*$_3$); ^{13}C NMR (75.5 MHz, C_6D_6) δ 151.20 (*C*HSi(OEt)$_2$O−), 59.15 (O*C*H$_2$CH$_3$), 18.36 (OCH$_2$*C*H$_3$); ^{29}Si NMR (79.5 MHz, ethanol) δ −56.15; high-resolution mass spectrometry (CI, ammonia) *m*/*z* calcd for $C_{10}H_{22}O_5Si_2$ + H 279.1084, found 279.1092.

*Cyclic Dimer (**5**).* A flask was charged with 1,1-bis(triethoxysilyl)ethene (20.5 g, 58.2 mmol), aqueous HCl (1.57 mL, 1 N, 87.3 mmol H_2O), and ethanol (145 mL). After stirring of the solution for 24 h and refluxing for 3 h, the solvent was removed in vacuo. Distillation of the crude oil under vacuum yielded 5.2 g (32%) of **5** with purity >84% by GC: bp 120−130 °C/50 μm; ^{1}H NMR (300 MHz, C_6D_6) δ 6.84 (s, 2 H, C*H*$_2$), 3.90 (q, 8 H, J = 7.0 Hz, OC*H*$_2$CH$_3$), 1.20 (t, 12 H, J = 7.0 Hz, OCH$_2$C*H*$_3$); ^{13}C NMR (75.5 MHz, C_6D_6) δ 149.21 (*C*H$_2$), 139.34 {*C*[Si(OEt)$_2$O−]$_2$}, 58.69 (O*C*H$_2$CH$_3$), 18.38 (OCH$_2$*C*H$_3$); ^{29}Si NMR (79.5 MHz, CD$_3$CD$_2$OD) δ −66.11; high-resolution mass spectrometry (CI, ammonia) *m*/*z* calcd for $C_{20}H_{44}O_{10}Si_4$ + NH$_4$ 574.2355, found 574.2350.

Sol−Gel Processing. *Characterization of Xerogels.* Solid-state ^{13}C and ^{29}Si (cross polarization magic angle spinning; CP MAS NMR) were performed on a Bruker AMX-400 MHz spectrometer at 100.63 and 79.5 MHz, respectively. The ^{29}Si CP MAS NMR spectra were deconvoluted using a Lorentz−Gaussian (50:50) fit. Surface area analyses were conducted with a Quantachrome Autosorb6 multiport nitrogen porosimeter. The samples were coated with 100−200 Å chrome using a Gatan model 681 high-resolution ion beam coater. These were analyzed using a high-resolution Hitachi S4500 field emission scanning electron microscope. Secondary electron images were taken using 5 kV accelerating voltage. The images were acquired digitally from the SEM using a PGT Imix imaging system.

Preparation of Ethenylene-Bridged Polysilsesquioxane Gels in Ethanol. *General Procedure for Gel Processing.* In each sol−gel polymerization, the monomer concentration was 0.4 M and the solutions were sealed in polypropylene bottles after mixing the monomer and catalyst solutions. Gelation was determined by the point at which the solution would not flow. After gelation, the polymers were aged for 2 weeks. The gels were then crushed and washed with H_2O (3 × 100 mL) and ether (2 × 50 mL) and dried under vacuum for 24 h at 100 °C.

1A. A solution of **1** (1.41 g, 4.00 mmol) in dry ethanol (4 mL) was mixed with a second solution of aqueous HCl (0.43 mL, 1 N, 23.9 mmol H_2O) in dry ethanol (4.0 mL), and the final volume was brought to 10.0 mL with additional ethanol. Gelation occurred after 5 days. White glassy gel fragments were obtained (550 mg, 106%): IR (KBr pellet) 3449, 3024, 2976, 1638, 1195, 1052, 908, 796 cm^{-1}; ^{13}C CP MAS NMR (50.20 MHz) δ 146 (*C*HSi(O−)$_3$), 58 (O*C*H$_2$CH$_3$), 17 (OCH$_2$*C*H$_3$); ^{29}Si CP MAS NMR (39.65 MHz) δ −63.8, −73.0, −81.4; BET surface area = 329 m^2/g, average pore diameter = 24 Å.

1B. A solution of **1** (1.41 g, 4.00 mmol) in dry ethanol (4 mL) was mixed with an ethanol (4.0 mL) solution of aqueous NaOH (0.43 mL, 1 N, 23.9 mmol H_2O), and the final volume was brought to 10.0 mL with additional ethanol. Gelation occurred in 23 min. White glassy gel fragments were obtained (525 mg, 101%): IR (KBr pellet) 3446, 2921, 2851, 1732, 1650, 1194, 1056, 927, 801, 430 cm^{-1}; ^{13}C CP MAS NMR (50.20 MHz) δ 146 (*C*HSi(O−)$_3$), 58 (O*C*H$_2$CH$_3$), 17 (OCH$_2$*C*H$_3$); ^{29}Si CP MAS NMR (39.65 MHz) δ −63.7, −73.4, −82.2; BET surface area = 600 m^2/g, average pore diameter = 23 Å.

2A. To a solution of **2** (705 mg, 2.0 mmol) in ethanol (2 mL) was added aqueous HCl (0.216 mL, 1 N, 12.0 mmol H_2O) dissolved in ethanol (2 mL), and the final volume was brought to 5.0 mL with additional ethanol. A rigid gel formed after 5 days. Opaque monolithic fragments were obtained (302 mg, 116%): IR (KBr pellet) 3647, 2921, 2851, 1731, 1652, 1462, 1357, 1147, 1100, 1037, 802, 654, 433 cm^{-1}; ^{13}C CP MAS NMR (50.20 MHz) δ 145.2 (*C*HSi(O−)$_3$), 58.9 (O*C*H$_2$CH$_3$), 17.0 (OCH$_2$*C*H$_3$); ^{29}Si CP MAS NMR (39.65 MHz) δ −73.5, −98.5; BET surface area = 447 m^2/g, average pore diameter = 22 Å.

2B. An ethanol (2 mL) solution of **2** (705 mg, 2.0 mmol) was mixed with aqueous NaOH (0.216 mL, 1 N, 12.0 mmol H_2O) dissolved in ethanol (2 mL), and the final volume was brought to 5.0 mL with additional ethanol. A white powder precipitated in less than 1 min after mixing. A fine white powder was recovered (177 mg, 68%): IR (KBr pellet) 3647, 2964, 1655, 1353, 1104, 1042, 811, 659, 526 cm^{-1}; ^{13}C CP MAS NMR (50.20 MHz) δ 145.5 (*C*HSi(O−)$_3$), 58.9 (O*C*H$_2$CH$_3$), 17.0 (OCH$_2$*C*H$_3$); ^{29}Si CP MAS NMR (39.65 MHz) δ −78.6; BET surface area = 473 m^2/g, average pore diameter = 47 Å.

3B. An ethanol (4 mL) solution of **3** (1.41 g, 4.00 mmol) was mixed with aqueous NaOH (0.43 mL, 1 N, 23.9 mmol H_2O) dissolved in ethanol (4 mL), and the final volume was brought to 10.0 mL with additional ethanol. The solution immediately became cloudy. After 9 months, a rigid cloudy gel had formed. Opaque monolithic fragments were obtained (390 mg, 75%): IR (KBr pellet) 3464, 3033, 2947, 1633, 1584, 1431, 1171, 1051, 866, 786, 501 cm^{-1}; ^{13}C CP MAS NMR (50.20 MHz) δ 149.0 [*C*H$_2$=C(Si(O−)$_3$)$_2$], 139.8 [CH$_2$=*C*(Si(O−)$_3$)$_2$], 59.0 (O*C*H$_2$CH$_3$), 17.2 (OCH$_2$*C*H$_3$); ^{29}Si CP MAS NMR (39.65 MHz) δ −62.0, −70.9, −78.9; BET surface area = 631 m^2/g, average pore diameter = 62 Å.

Preparation of Ethenylene-Bridged Polysilsesquioxane Gels in THF. ***1A-THF.*** A THF solution of **1** (705 mg, 2.00 mmol) and aqueous HCl (0.216 mL, 1 N, 12.0 mmol H_2O) became cloudy within 5 min of mixing, and a gel formed after 4 h. Monolithic gel fragments were obtained (274 mg, 105%): IR (KBr pellet) 3449, 2976, 1638, 1194, 1123, 1050, 909, 795, 433 cm^{-1}; ^{13}C CP MAS NMR (50.20 MHz) δ 146.0 (*C*HSi(O−)$_3$); ^{29}Si CP MAS NMR (39.65 MHz) δ −64.4, −73.3, −82.1; BET surface area = 379 m^2/g, average pore diameter = 22 Å.

1B-THF. A THF solution of **1** (705 mg, 2.00 mmol) and aqueous NH_3 (0.216 mL, 1 N, 12.0 mmol H_2O) gradually became opaque after mixing, and a gel formed after 2 days. Monolithic gel fragments were recovered (274 mg, 105%): IR (KBr pellet) 3646, 2956, 1655, 1314, 1195, 1123, 1052, 914, 786 cm^{-1}; ^{13}C CP MAS NMR (50.20 MHz) δ 145.8 (*C*HSi(O−)$_3$); ^{29}Si CP MAS NMR (39.65 MHz) δ −64.4, −73.6, −82.6; BET surface area = 726 m^2/g, average pore diameter = 24 Å.

2A-THF. A THF solution of **2** (705 mg, 2.00 mmol) and aqueous HCl (0.216 mL, 1 N, 12.0 mmol H_2O) gelled 10 days after mixing. Monolithic gel fragments were recovered (290 mg, 112%): IR (KBr pellet) 3646, 2956, 1733, 1630, 1356, 1128, 1033, 920, 808, 655, 517 cm^{-1}; ^{13}C CP MAS NMR (50.20 MHz) δ 145.6 (*C*HSi(O−)$_3$), 58.9 (O*C*H$_2$CH$_3$), 17.0 (OCH$_2$*C*H$_3$); ^{29}Si CP MAS NMR (39.65 MHz) δ −72.4, −98.5; BET surface area = 307 m^2/g, average pore diameter = 24 Å.

Table 1. Sol−Gel Polymerization Conditions[a] and Gel Times for Monomers 1−3

monomer (catalyst)	solvent (EtOH)	solvent (THF)
1 (acid[b])	clear gel in 5 days	cloudy gel in 4 h
1 (base[c])	clear gel in 23 min	opaque gel in 2 days
2 (acid[b])	clear gel in 5 days	clear gel in 10 days
2 (base[c])	ppt immediately	ppt in 2 h
3 (acid[b])	no gel after 1 year	
3 (base[c])	cloudy gel in 9 months	

[a] All polymerizations were performed with a monomer concentration of 0.4 M, 6 equiv of water, and 10.8 mol % catalyst. [b] The acid was 1 N HCl. [c] The base was 1 N NaOH in EtOH and 1 N NH_3 in THF.

2B-THF. A THF (2 mL) solution of **2** (705 mg, 2.0 mmol) was mixed with aqueous NH_3 (0.216 mL, 1 N, 12.0 mmol H_2O) dissolved in THF (2 mL), and the final volume was brought to 5.0 mL with additional THF. A white powder precipitated after 2 h. A fine white powder was recovered (189 mg, 73%): IR (KBr pellet) 3449, 2962, 1630, 1353, 1130, 1040, 807, 657, 526 cm^{-1}; ^{13}C CP MAS NMR (50.20 MHz) δ 144.5 ($CHSi(O-)_3$); ^{29}Si CP MAS NMR (39.65 MHz) δ −78.1; BET surface area = 742 m^2/g, average pore diameter = 46 Å.

Results and Discussion

Monomer Synthesis. A mixture of *E*-monomer (**1**) and vinylidene monomer (**3**) was produced by the reaction of triethoxyvinylsilane with $RuCl_2(PPh_3)_2$.[10,11] Spinning band distillation of the mixture (84:16 **1**/**3**) yielded a distillate that was enriched in **3**, and the material remaining in the boiling flask was pure **1**. Pure **3** was obtained by a second spinning band distillation of the enriched fractions. Photochemical isomerization of **1** was utilized to produce a mixture of **1** and *Z*-monomer **2** (74:26, respectively), and again consecutive spinning band distillations were required to purify **2**. Although the overall isolated yield of **2** from a single photolysis reaction was low (10%), **1** was recovered from the distillations and recycled into the photolysis reaction to prepare more of the *Z*-monomer.

Sol−Gel Polymerizations. Monomers **1**−**3** exhibit remarkably different gelation behavior under identical sol−gel polymerization conditions. Acid-catalyzed polymerizations of ethanol solutions (0.4 M) of monomers **1** and **2** produce rigid transparent gels in 5 days (Table 1). However, when THF is utilized as the solvent in the same polymerizations, **1** forms a cloudy white gel in 4 h while **2** requires 10 days to set up as a rigid colorless transparent gel. Contrasting sharply with **1** and **2**, the vinylidene monomer **3** is apparently extremely resistant toward polymerization; under identical acidic sol−gel conditions, the monomer does not form a gel or a precipitate even after 1 year!

When basic conditions are employed, slightly opaque rigid free-standing gels can be produced from **1** in 20 min (EtOH) or 36 h (THF). In the presence of a basic catalyst, monomer **2** reacts very rapidly to produce a white precipitate in both EtOH and THF as gels could not be obtained under these conditions. Again, **3** is very slow to polymerize with gelation occurring only after 9 months in EtOH with NaOH catalyst. Since the reaction conditions employed are the same for each monomer, the observed differences in polymerization behavior must stem from the differences in the orientation of the triethoxysilyl moieties within each monomer. It was suspected that intramolecular cyclic condensation reactions could play a significant role in the oligomerization of **2** and **3** while this seemed unlikely in **1** due to its trans configuration. Thus, the early condensation reactions and the structures of the initial oligomers were studied to determine the impact of cyclic silsesquioxanes on the formation of ethenylene-bridged polysilsesquioxane gels.

^{29}Si NMR Studies. ^{29}Si NMR chemical shifts are a sensitive diagnostic for Baeyer strain in rings containing silicon atoms making ^{29}Si NMR spectroscopy a useful tool for determining if smaller (4−7-membered rings) cyclics are present during a sol−gel polymerization reaction. With decreasing ring size, reduced bond angles at silicon give rise to a marked downfield shift in the δ_{Si}.[9,12,13] Strained rings aside, there are four types of silicon centers present during the sol−gel polymerization of organotrialkoxysilanes since there may be from 0 to 3 siloxane bonds at any one silicon atom. These silicon atoms are considered to be trifunctional with respect to the alkoxide ligands and are denoted as T^n, which is a modification of the General

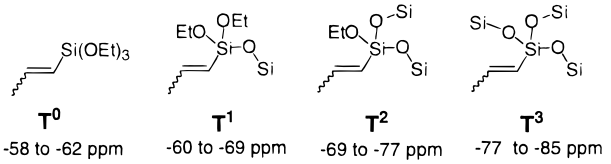

Electric Q notation.[14] The superscript *n* represents the number of siloxane bonds to a particular silicon atom. The chemical shift for a silicon center is progressively shifted upfield approximately 5−10 ppm with each acyclic condensation making each type of silicon easily distinguishable in the ^{29}Si NMR spectrum. In contrast, hydrolysis causes a shift downfield of about 1−2 ppm with each substitution of an ethoxide with a hydroxyl group. Thus, the ^{29}Si NMR spectra for the early hydrolysis and condensation reactions of alkyl triethoxysilanes exhibits a complex set of peaks that can be used to follow the progress of the sol−gel polymerization reactions.

Monitoring the change in populations of silicon species with different degrees of condensation over time is generally successful for acid-catalyzed sol−gel polymerizations. Under basic conditions, the rates of hydrolysis and condensation of alkoxysilanes *increase* as the silicon center becomes more hydrolyzed and condensed. Thus the initial condensation products are difficult to observe as they quickly react to form polymer under basic conditions.[14] In contrast, hydrolysis and condensation rates *decrease* with increasing degree of condensation at silicon under acidic conditions permitting ^{29}Si NMR spectra to be readily obtained for the acid-catalyzed hydrolysis and condensation of **1**−**3** (0.4 M) in ethanol with 1 or 2 equiv of H_2O and 1.8 or 3.6 mol % HCl as catalyst. Under these conditions, hydrolysis and condensation products of ethoxysilanes can be easily moni-

(12) Englehardt, G.; Jancke, H.; Magi, M.; Pehk, T.; Lippmaa, E. *J. Organomet. Chem.* **1971**, *28*, 293.
(13) Burton, D. J.; Harris, R. K.; Dodgson, K.; Pellow, C. J.; Semlyen, J. A. *Polym. Commun.* **1983**, *24*, 278.
(14) Brinker, C. J.; Scherer, G. W. *Sol−Gel Science: the physics and chemistry of sol−gel processing*, 1st ed.; Academic Press: San Diego, CA, 1990; p 160.

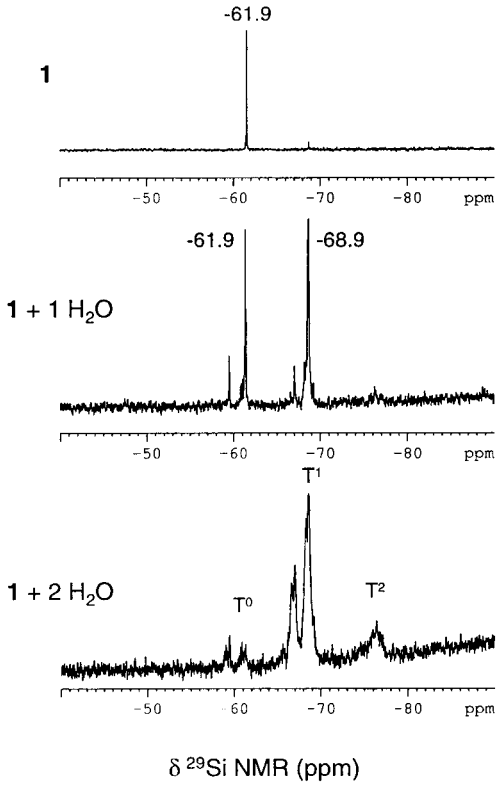

Figure 1. ^{29}Si NMR spectra of **1**, **1** + 1 equiv of H_2O, and of **1** + 2 equiv of H_2O, the latter two under acidic conditions.

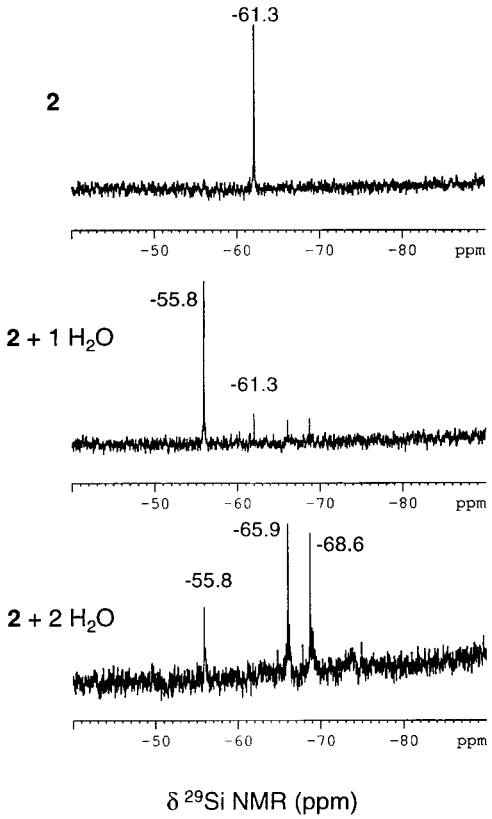

Figure 2. ^{29}Si NMR spectra of **2**, **2** + 1 equiv of H_2O, and of **2** + 2 equiv of H_2O, the latter two under acidic conditions.

tored over time, permitting not only kinetic measurements but structural information concerning the growth of the oligomeric species.

The acid-catalyzed reaction of **1** with 1 equiv of H_2O in ethanol after 4 h gave a ^{29}Si NMR spectrum (Figure 1) in which the single, double, and triple hydrolysis products of **1** were observed at −60.6, −59.2, and −58.7 ppm, respectively.[15] After 24 h the spectrum consisted of two main peaks of roughly equal intensity at −61.9 and −68.7 ppm. The chemical shift of −61.9 ppm is the same as that for unreacted monomer and must arise from T^0 silicon nuclei while the second signal is shifted 7.2 ppm upfield and is thus assigned to T^1 silicon nuclei. No T^2 or T^3 silicons are observed under the controlled hydrolysis and condensation reactions with 1 equiv of H_2O, indicating that no significant branching was occurring. This type of polymerization is expected under acidic conditions.[14] However, this does not rule out the possibility of large unstrained rings.

A single new peak at −55.8 ppm appears in the ^{29}Si NMR spectrum of **2** (ethanol) only minutes after adding 1 equiv of H_2O (1 N HCl) (Figure 2, middle). The *downfield* shift of the new silicon species is over 6 ppm from the signal (T^0) observed for **2** (δ = −61.3 ppm) which is much too large of a shift to be attributed to a hydrolysis product. The downfield shift is consistent with the presence of an intramolecular cyclization product (**4**) exhibiting Baeyer strain as shown in Scheme 3. If an acyclic condensation had occurred, a signal *upfield* from that of the starting monomer would be expected. The addition of 2 equiv of H_2O to **2** under acidic conditions gives rise to two new signals of equal intensity at −65.9 and −68.6 ppm with complete consumption of the remaining monomer and of the initial cyclic product **4** (δ_{Si} = −55.8 ppm). The $\Delta\delta$ of 2.7 ppm is too large for the two signals to be explained by one type of silicon compound and its single hydrolysis product. Thus, there appears to be two unique types of silicon atoms present after the addition of 2 equiv of H_2O. The intensities of the two signals remain equivalent over time suggesting that they arise from a single compound. An acyclic T^1 silicon would be expected to give rise to a signal around −69 ppm rather than the observed δ_{Si} of −65.9 ppm indicating that some type of strained cyclic product is probably present. The signal at −68.6 ppm could arise from an acyclic T^1 or a T^2 that is in a strained cyclic environment.

Scheme 3

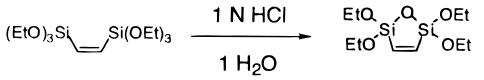

2 **4**

The same reaction conditions employed for **1** and **2** were repeated for **3** using 1 equiv of H_2O. Initially, only the hydrolysis products of **3** were observed in the ^{29}Si NMR spectrum. After 24 h, however, the dominant peak in the spectrum was observed at δ_{Si} = −66.1 ppm. The upfield shift of this condensation product from that of the monomer (δ_{Si} = −58.0 ppm) indicates that the T^1 silicon is not part of a *strained* cyclic system. No T^2 or T^3 silicons were observed.

Mass Spectrometry Studies. Mass spectrometric studies were carried out under conditions identical to those used in the NMR investigations so that the initial

(15) Similar ^{29}Si NMR chemical shifts for the hydrolysis and condensation products of vinyltriethoxysilane were reported by: Devreux, F.; Boilot, J. P.; Chaput, F.; Lecomte, A. *Phys. Rev.* **1990** *41*, 6901−10.

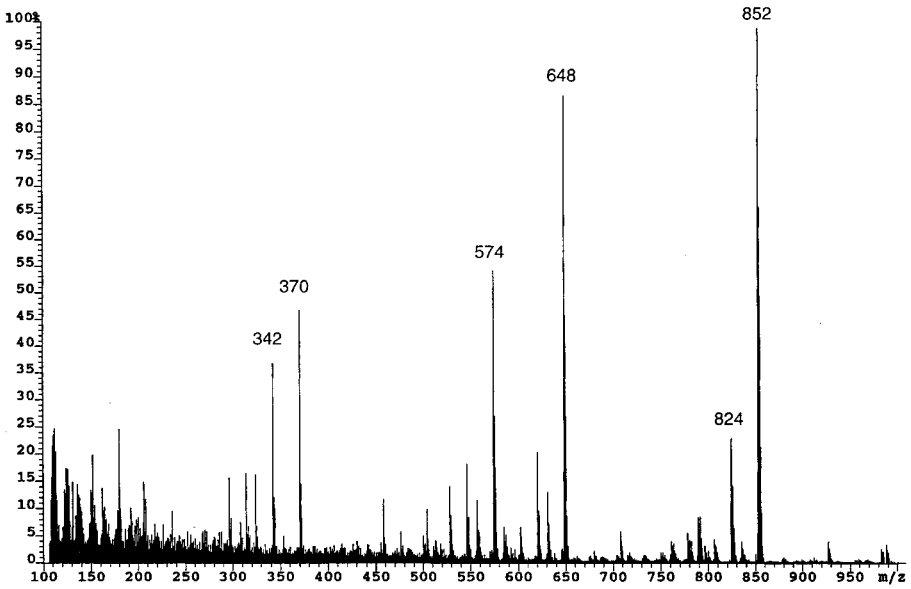

Figure 3. Mass spectrum of **1** after 19 h of reaction time with 1 equiv of H_2O under acidic conditions.

condensation products observed in the ^{29}Si NMR could be identified. By periodically observing the mass spectrum (CI MS, ammonia) over several hours, it was possible to discover not only what intermediates were involved but also how these products change with time providing a dynamic view of the oligomerization process.[16] The milder ionization conditions of chemical ionization mass spectrometry minimized fragmentation so that the mass spectra depict many of the parent ions of the species participating in the sol−gel polymerization reactions. For example, the mass spectra of **1**−**3** before the addition of aqueous catalyst showed the expected molecular ion peaks of *m*/*z* 353 $[M + H]^+$ and *m*/*z* 370 $[M + NH_4]^+$ along with fragment ions due to loss of ethoxide $[M - OEt]^+$. The mass spectrometric analyses of the hydrolysis and condensation reactions were conducted by mixing 1 equiv of water (1 N HCl) to solutions of **1**, **2**, or **3** in ethanol (0.4 M) and then removing samples by syringe for direct insertion into the mass spectrometer.

*Oligomerization of **1***. Monitoring of the reaction of **1** with 1 equiv of water containing 1.8 mol % aqueous HCl by periodically observing a mass spectrum of the mixture showed the gradual depletion of the monomer with concomitant increase in the concentration of dimers and trimers. After 19 h of reaction time, the majority of **1** had been converted into oligomers as shown in Figure 3. The dominant ion at *m*/*z* 852 is assigned to the cyclic trimer $[\mathbf{1t} + NH_4]^+$. The acyclic dimer is also observed at *m*/*z* 648 $[\mathbf{1d} + NH_4]^+$ as well as the cyclic dimer at *m*/*z* 574 $[\mathbf{1d} + NH_4]^+$. A small amount of monomer is still evident by the ion at *m*/*z* 370 $[\mathbf{1} + NH_4]^+$ and its single hydrolysis product at *m*/*z* 342. The mass spectral study of the hydrolysis and condensation of **1** shows a steady progression of the condensation products toward a polymer with a significant contribution from large, unstrained rings. Soon after hydrolysis, the monomer dimerizes to form the acyclic dimer. This dimer can then undergo an intramolecular condensation reaction to form **1d** or an additional intermolecular condensation to give the acyclic trimer, which then cyclizes to form the cyclic trimer. The structure proposed for the cyclic dimer **1d** is a 10-membered ring with two trans double bonds. This pattern of polymer growth is consistent by the ^{29}Si NMR spectrum (Figure 1) which is dominated by $\mathbf{T}^1$ silicons, consistent with a linear or unstrained cyclic structure, and shows only a minor contribution from $\mathbf{T}^2$ type silicons which would indicate a more branched structure. It is important to remember that these experiments monitoring the early sol−gel chemistry are conducted with only 1−2 equiv of water. Polymerization with greater amounts of water would permit more ethoxide groups to be hydrolyzed likely leading to more acyclic and branched structures.

*Oligomerization of **2***. The conditions used in the mass spectral study of **1** were repeated for **2**. After 10 min of reaction time, the major ion present in the mass spectrum is at *m*/*z* 296 and is assigned to the intramolecular cyclization product $[\mathbf{4} + NH_4]^+$ which was observed in the ^{29}Si NMR studies (Scheme 3). To confirm the identity of **4**, the intramolecular cyclization product was synthesized in THF by the reaction of **2** with 1 equiv of water (1 N HCl). The product was isolated by vacuum distillation, and the ^{1}H, ^{13}C, and ^{29}Si NMR spectra were all consistent with the structure of **4**. In particular, the δ_{Si} of −56.2 ppm which is shifted significantly downfield from that of **2** ($\delta_{Si} = -61.9$ ppm) verifies the presence of **4** since a downfield shift is expected in a strained cyclic structure. In an analogous system, a downfield shift of 8.6 ppm is observed in the ^{29}Si NMR spectrum for 2,2,5,5-tetramethyl-2,5-disilaoxacyclopentane obtained from the intramolecular cyclization of 1,2-bis(dimethylethoxysilyl)ethane.[17] The reaction proceeds smoothly in THF to a near quantitative

(16) This technique has been successfully used to determine the initial oligomers formed from the hydrolysis and condensation of tetramethoxysilane (Campostrini, R.; Carturan, G.; Pelli, B.; Traldi, P. *J. Non-Cryst. Solids* **1989**, *108*, 143) and α,ω-bis(triethoxysilyl)-alkanes.[9]

(17) The chemical shift difference was obtained from a comparison of an authentic sample of 1,2-bis(dimethylethoxysilyl)ethane with a literature value of the intramolecular cyclization product: Seyferth, D.; Robison, J. *Macromolecules* **1993**, *26*, 407.

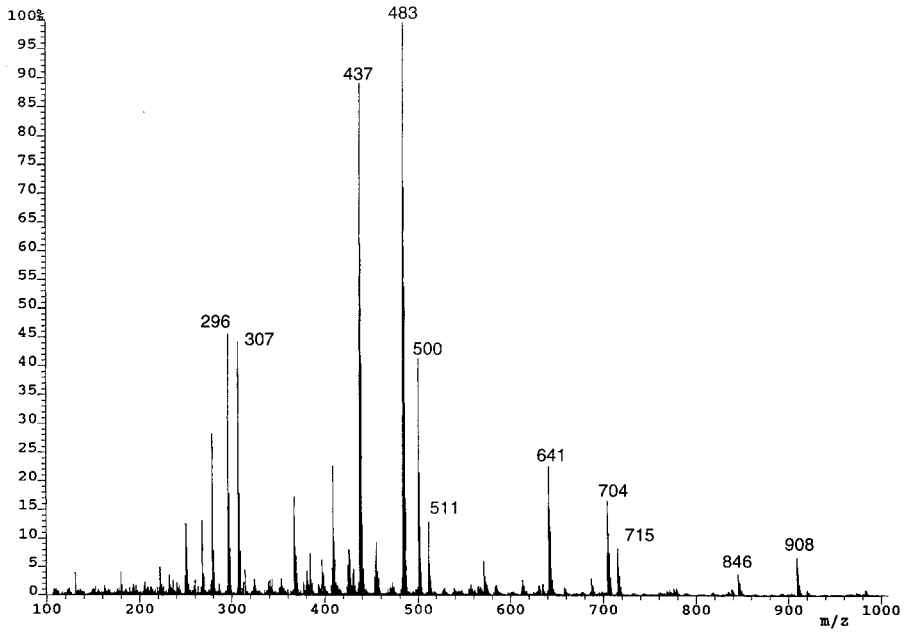

Figure 4. Mass spectrum of **2** after 22 h of reaction time with 1 equiv of H_2O under acidic conditions.

Scheme 4

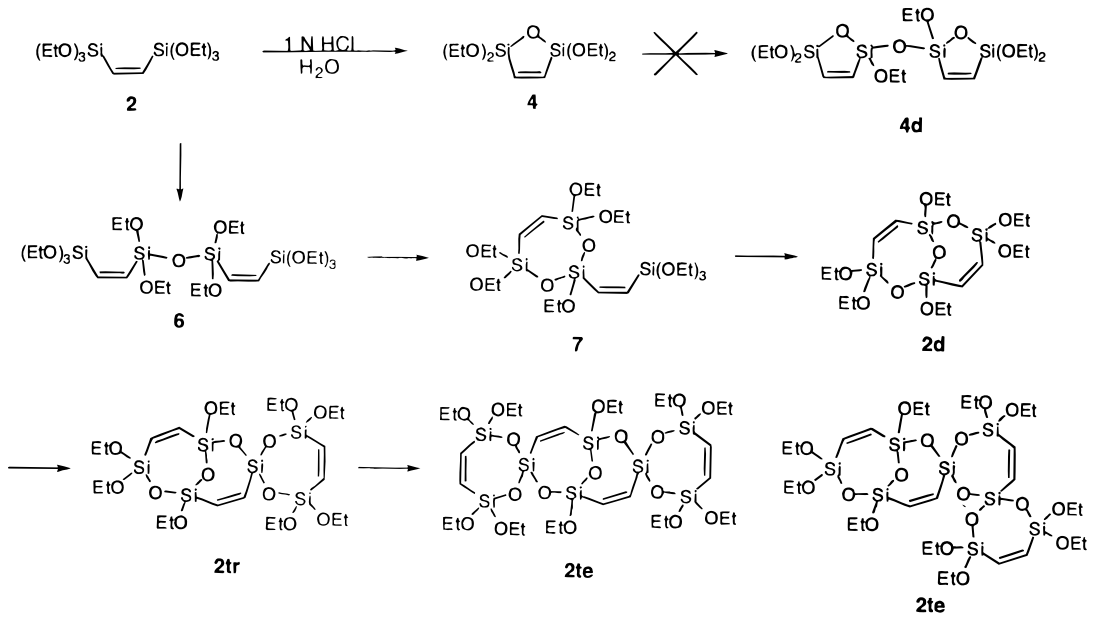

conversion of **2** to **4**; however, when the reaction is performed in ethanol, a mixture of **2**, **4**, and oligomers of **2** is obtained.

The mass spectrum of the reaction of **2** with aqueous HCl in ethanol after 22 h is dominated by a family of peaks with ion masses of *m*/*z* 409−500 (Figure 4). All of these ions are assigned to the formation of a bicyclic dimer (**2d**) consisting of two fused seven-membered rings. The rapid formation of seven-membered rings has been observed previously in the intramolecular cyclization of 1,4-bis(triethoxysilyl)butane.[9] The bicyclic dimer **2d** is represented by the ions at *m*/*z* 500 [**2d** + NH_4]$^+$ and 483 [**2d** + H]$^+$ and a fragmentation product at *m*/*z* 437 [**2d** − OEt]$^+$. The peak at *m*/*z* 409 is due to the fragmentation of the single hydrolysis product of **2d**.

It could be argued that the series of ions with *m*/*z* 409−500 arise from the dimerization of **4** without ring opening as shown in Scheme 4. However, this type of dimer would be inconsistent with the observations in the ^{29}Si NMR of the hydrolysis and condensation of **2**. In the NMR studies, **4** ($\delta_{Si} = -55.8$ ppm) is replaced by a product with two peaks of equivalent intensities at −65.9 and −68.6 ppm. If **4d** was the condensation product, two signals would be expected, but a signal around −56 ppm would still be expected from the two T^1 silicons present in the five-membered rings. However, the signals at −65.9 and −68.6 ppm are in the expected range for the T^1 and T^2 silicons present in **2d** since these silicons are part of an expanded ring system that is not as strained as **4**. Also, there is an ion in the mass spectrum with *m*/*z* 511 [**7** − OEt]$^+$ which can best be explained as a fragmentation product of **7**. This type of intermediate is expected in the formation of **2d** as outlined in Scheme 4. Intermediate **6** is not observed in the mass spectrum probably due to a very rapid intramolecular cyclization to form **7**.[9] With the confor-

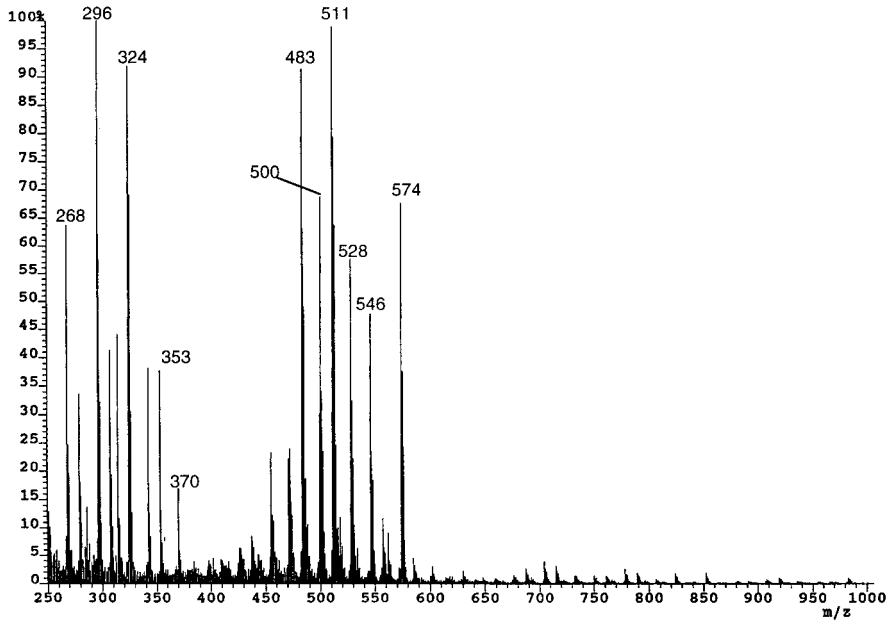

Figure 5. Mass spectrum of **3** after 20 h of reaction time with 1 equiv of H_2O under acidic conditions.

mational freedom restricted in **7** compared to that of **6**, the second intramolecular cyclization to form **2d** may not be as rapid allowing the observation of a small concentration of this intermediate in the mass spectrum.

In addition to the bicyclic dimer **2d**, molecular ions representing trimers and tetramers of **2** are observed in the mass spectrum. A variety of acyclic and cyclic structures were examined to explain the ions observed at masses of $m/z = 641$ and higher. We tentatively assign these ions to the tricyclic trimer and to the two possible tetrameric structures shown in Scheme 4. The peaks with m/z 704 [**2tr** + NH_4]$^+$ and 687 [**2tr** + H]$^+$ are assigned to the parent peaks of a trimer of **2**, and a fragmentation product is observed at m/z 641 [**2tr** − OEt]$^+$. The parent peak for the tetramer of **2** (Scheme 4) is observed at m/z 908 [**2te** + NH_4]$^+$, and a fragmentation product of this tetramer, at m/z 846 [**2te** − OEt]$^+$. No acyclic structures could be postulated that were consistent with the observed ions. The proposed trimer and tetramer would be formed by the cyclic condensation of monomer with the T^1 silicons of **2d**. The identification of the oligomers of **2** by ^{29}Si NMR and mass spectral studies demonstrates the propensity of this monomer to form cyclic condensation products, preferentially seven-membered rings. This is in sharp contrast to the oligomerization of **1** which exhibited strictly unstrained acyclic or large cyclic condensation products. *The persistence of the seven-membered rings suggests that they may be incorporated into the final structure of the polymeric gels.*

*Oligomerization of **3**.* Ten minutes after the addition of the aqueous HCl to a solution of **3**, the mass spectrum revealed the expected single and double hydrolysis products. In the same mass spectrum, a small concentration of dimers with masses from $m/z = 455-585$ were observed. The reaction was followed for several hours, and during this time, the relative intensity of the peaks in this region continued to grow. After 20 h, the only families of peaks present were those of the monomer and dimer (Figure 5). No major peaks with masses $m/z = 600-1000$ were observed indicating the absence of any significant concentrations of trimer or tetramer.

All of the major ions observed with m/z between 483 and 574 after 20 h of reaction can be attributed to the formation of a cyclic dimer (**5**). The parent ions for this species occur at m/z 574 [**5** + NH_4]$^+$ and 557 [**5** + H]$^+$. The peak at $m/z = 546$ was assigned to the [M + NH_4]$^+$ ion from the first hydrolysis product of **5**. The peak at $m/z = 500$ was attributed to the [M + NH_4]$^+$ ion from the bicyclic dimer resulting from condensation across the ring. Peaks at $m/z = 511$ and 483 were assigned to the fragmentation ions [M − OEt]$^+$ of **5** and of its hydrolysis products.

The formation of **5** is consistent with the observed stability of eight-membered siloxane rings in the hydrolysis and condensation of dihalodimethylsilanes.[18,19] The resistance of this structure to reacting and forming higher oligomers appears to be the bottleneck in the polymerization of **3** that causes the lengthy times for gelation (Table 1). Despite the presence of large amounts of hydrolyzed **3** and **5**, neither the homocondensation of **5** nor the heterocondensation of **3** and **5** is observed to any appreciable extent since no major ions are observed with m/z between 600 and 1000.

A small amount of **5** can actually be isolated from the hydrolysis and condensation of **3**. The yield of **5** was maximized by optimizing the reaction conditions and the amount of water (1.5 equiv) introduced into the reaction. The cyclic dimer was distilled from the reaction mixture to yield **5** in a purity of about 85%. Further purification of this product was complicated by the presence of hydrolysis products of **5**. The ^{1}H, ^{13}C, and ^{29}Si NMR spectra were all consistent with the proposed dimeric structure of **5**, and the δ_{Si} of −66.1 observed for this isolated product is identical to that observed in the ^{29}Si NMR hydrolysis and condensation studies of **3**.

The sol−gel polymerization studies of monomers **1**−**3** reveal unique reactivity patterns for each monomer under acidic conditions. Acyclic linear chains and large rings predominate in the polymerization of **1** while the hydrolysis and condensation of **2** is characterized by the

(18) Rochow, E. G.; Gilliam, W. F. *J. Am. Chem. Soc.* **1941**, *63*, 798.
(19) Cypryk, M.; Sigwalt, P. *Macromolecules* **1994**, *27*, 6245−53.

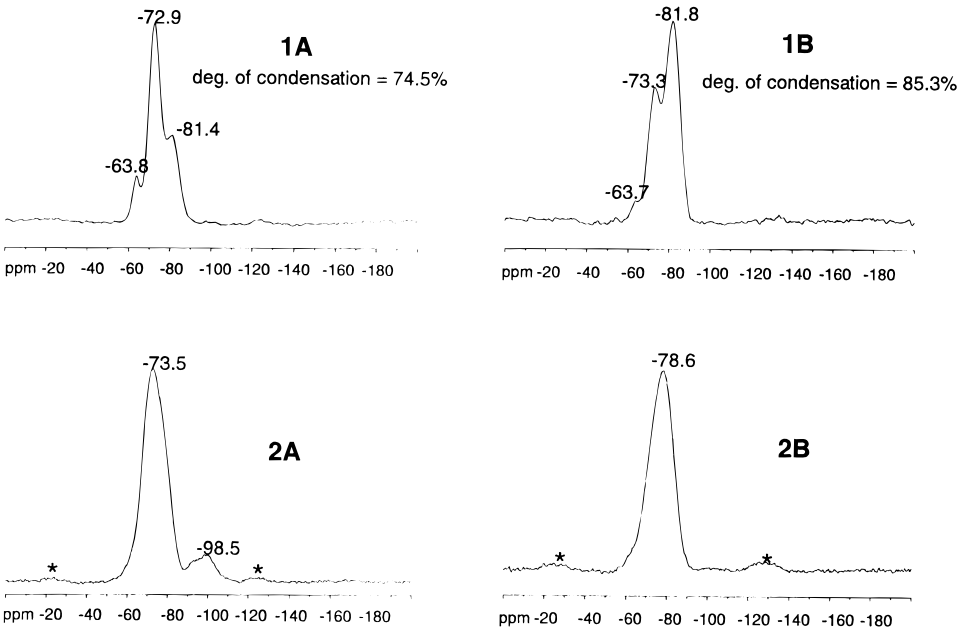

Figure 6. ^{29}Si CP MAS NMR spectra of xerogels **1A**, **1B**, **2A**, and **2B**. Peaks labeled with an asterisk are spinning sidebands.

formation of seven-membered rings to build up the polymer network. Polymerization of **3** is apparently inhibited by the formation of the cyclic dimer **5** which is resistant to further condensation reactions. Determining if the cyclics are involved in the formation of gels from the polymerization of **1**−**3** under basic conditions is complicated because the rate of condensation reactions are too fast to follow with ^{29}Si NMR and only T^3 silicons are observed.

Characterization of Xerogels. Due to the difficulty in polymerizing **3** to a highly condensed xerogel, most of the analytical data was obtained for xerogels prepared from monomers **1** and **2**. To understand what effect the orientation of the silicon moieties have on the final properties of the materials, the xerogels were characterized by solid-state NMR, nitrogen sorption porosimetry, and scanning electron microscopy.

Solid-State ^{13}C and ^{29}Si NMR. Solid-state NMR was utilized to investigate the chemical environment surrounding each silicon and the chemical structure of each xerogel at the molecular level. The ^{13}C CP/MAS NMR spectra of all the xerogels prepared from **1** and **2** are relatively simple and are characterized by a strong resonance at 146 ppm representing the carbons in the ethenylene bridge. As expected, two peaks are observed in the olefinic region of the ^{13}C CP/MAS NMR of xerogel **3B** at −149 and −139 ppm. The only other signals present in all of the materials are from unhydrolyzed residual ethoxide groups, identified by peaks at about 58 and 17 ppm, which are present in all of the materials except **1B** and **2B-THF**.

Distinct differences between the polymers prepared from **1** and **2** are observed in the ^{29}Si CP/MAS NMR spectra. Typically, for arylene- or alkylene-bridged polysilsesquioxanes, there are three types of silicon[20] (T^1, T^2, and T^3) present which are distinguishable in the ^{29}Si CP/MAS NMR spectrum, and the concentrations of each species can be evaluated and a degree of condensation determined.[3] The overlapping T^1, T^2, and T^3 silicons are easily discernible in the ^{29}Si NMR spectrum of the polymers prepared from **1** (Figure 6). Consistent with observations in other organically bridged polysilsesquioxanes and in sol−gel derived silicas, the degree of condensation in materials which were polymerized utilizing an acidic catalyst (75%) is lower than when a basic catalyst (85%) is employed.[3,4,14] Xerogel **3B** exhibits a ^{29}Si CP/MAS NMR spectrum similar to the spectra for the materials prepared from **1**. The expected silicon resonances are observed at −62.0, −70.9, and −78.9 ppm, and the degree of condensation was calculated to be 78%. The value for the degree of condensation of **3B** is lower than those for the base-catalyzed gels produced from **1**. No Q silicons are observed in the spectra indicating that the ethenylene bridge in **1** and the vinylidene bridge in **3** are not hydrolyzed during the polymerization reactions.

^{29}Si CP/MAS NMR spectra of the polysilsesquioxanes derived from **2** lack the resolution observed in the spectra of xerogels prepared from **1** (Figure 6). A single broad peak with no obvious shoulders extends over the entire region where the signals for the T^1, T^2, and T^3 silicons are expected.[21] The observation of a single broad peak suggests that the three types of silicon exist in a significantly different chemical environment compared to those observed for xerogels of **1**. From the mass spectral studies of the early condensation reactions involved in the polymerization of **2**, a propensity to form seven-membered rings was observed. A variety of T^2 and T^3 silicons in chemically different environments are possible in a network assembled from the cyclic structures identified in the oligomerization of **2**. The presence of silicons in acyclic environments formed during the synthesis of the polymer or from ring opening during drying would also add to the variety of chemically different silicons. A combination of all these factors is most likely responsible for the poor resolution

(20) Usually T^0 silicons are not observed in the ^{29}Si CP/MAS NMR of polysilsesquioxanes.

(21) Abe, Y.; Namiki, T.; Tsuchida, K.; Nagao, Y.; Misono, T. *J. Non-Cryst. Solids* **1992**, *147/148*, 47.

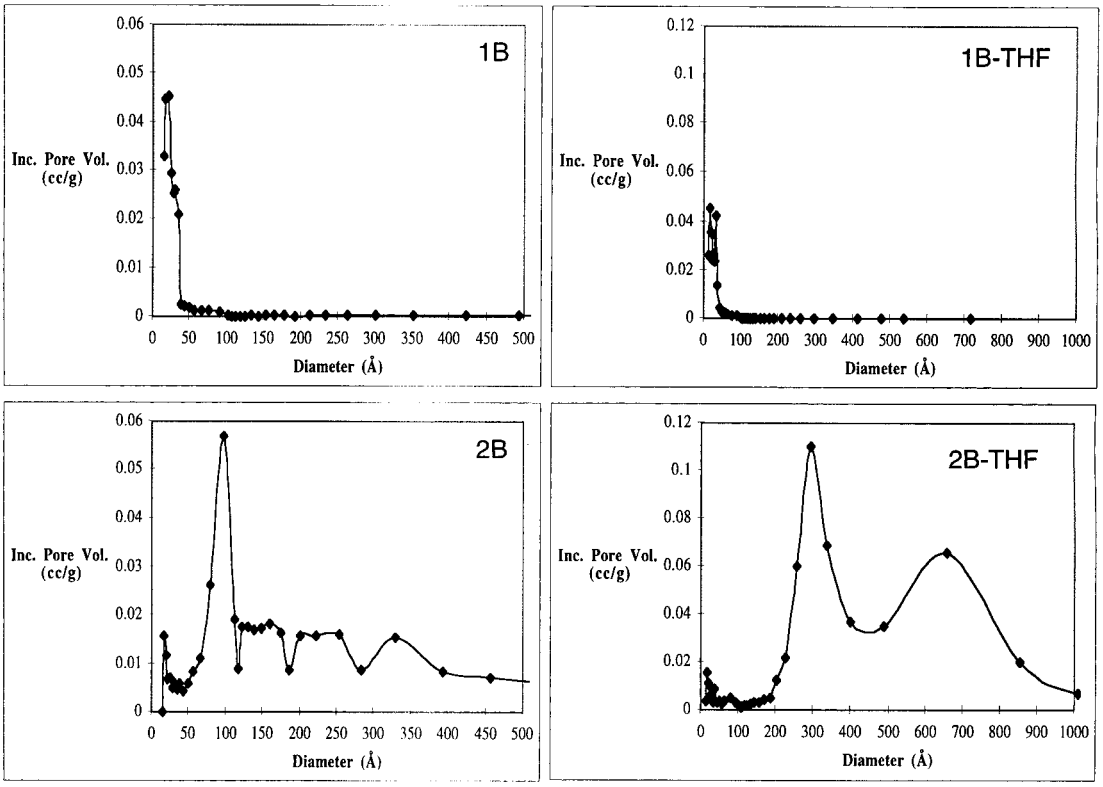

Figure 7. Incremental pore volume plots of xerogels **1B**, **1B-THF**, **2B**, and **2B-THF** determined by nitrogen sorption porosimetry.

observedin the ^{29}Si CP/MAS NMR spectra of the xerogels produced from **2**.

The center of the broad peak observed in the xerogels produced under basic conditions (**2B** and **2B-THF**) is shifted about 5 ppm upfield from the corresponding signal in the acid-catalyzed xerogels (**2A** and **2A-THF**). There are two possible explanations for the chemical shift difference in the materials. The base-catalyzed xerogels could be more highly condensed containing a higher concentration of T^3 silicons which would be consistent with the observations in the polymerization of **1**. The chemical shift difference could also arise from the presence of a larger concentration of silicon nuclei in acyclic environments in the base-catalyzed materials reducing the amount of Baeyer strain in the system. In both acid-catalyzed xerogels, **2A** and **2A-THF**, a small peak at −99 ppm is also observed in the ^{29}Si CP/MAS NMR that is assigned to a small amount of silica (Q) species present in the material. This indicates that a small amount of silicon−carbon bond cleavage is occurring during the acid-catalyzed sol−gel polymerization of **2**.[22]

Porosimetry. Examination of the porosities of the xerogels prepared from monomers **1**−**3** revealed a profound dependence of pore structure on the substitution geometry of the monomer. Nitrogen sorption porosimetry was utilized to evaluate the pore structure and surface area of each xerogel. The surface areas were determined by the multipoint BET method and are tabulated along with mean pore diameters (BJH) and pore volumes in Table 2.[23] Most of the ethenylene-bridged polysilsesquioxanes are characterized by a small

Table 2. Summary of Surface Areas and Pore Diameters Determined by Nitrogen Sorption Porosimetry for Materials Prepared from 1−3

xerogels	BET surf areas[a] (m^2/g)	av pore diam.[b] (Å)	pore vol (cm^3/g)
1A	352	22	0.190
1B	691	22	0.387
2A	447	22	0.248
2B	473	47	0.561
3B	631	62	0.973
1A-THF	379	22	0.206
1B-THF	779	24	0.466
2A-THF	307	24	0.180
2B-THF	742	46	0.850

[a] Surface areas determined using the multipoint BET (Brunauer−Emmett−Teller) method. The P/P_o range was $0.05 \leq P/P_o \leq 0.35$. [b] The average pore diameter was calculated from $d_{av} = 2(2V/S)$, where V is the volume of liquid nitrogen contained in the pores and S is the BET surface area.

average pore diameter of 22−24 Å. However, the xerogels that formed after **2** polymerized and then precipitated under basic conditions had average pore diameters of 46−47 Å and xerogel **3B** had an average pore diameter of 62 Å. A general trend in the ethenylene-bridged polysilsesquioxanes is that xerogels prepared using a basic catalyst exhibit much higher surface areas (473−779 m^2/g) than those prepared with an acid catalyst (307−447 m^2/g).

A more meaningful description of the porosity of a material than the average pore diameter can be obtained from a plot of the incremental pore volume distributions. These plots are prepared from the desorption branch of the nitrogen isotherm. If one starts from the point at which all pores are filled, the relative pressure is lowered incrementally. At each increment, the volume of nitrogen removed is measured and a pore diameter is calculated from the relative pressure using

(22) Henry, C.; Brook, M. A. *Tetrahedron* **1994**, *50*, 11379−90.
(23) Gregg, S. J.; Sing, K. S. W. *Adsorption, Surface Area, and Porosity*, 2nd ed.; Academic Press: London, 1982.

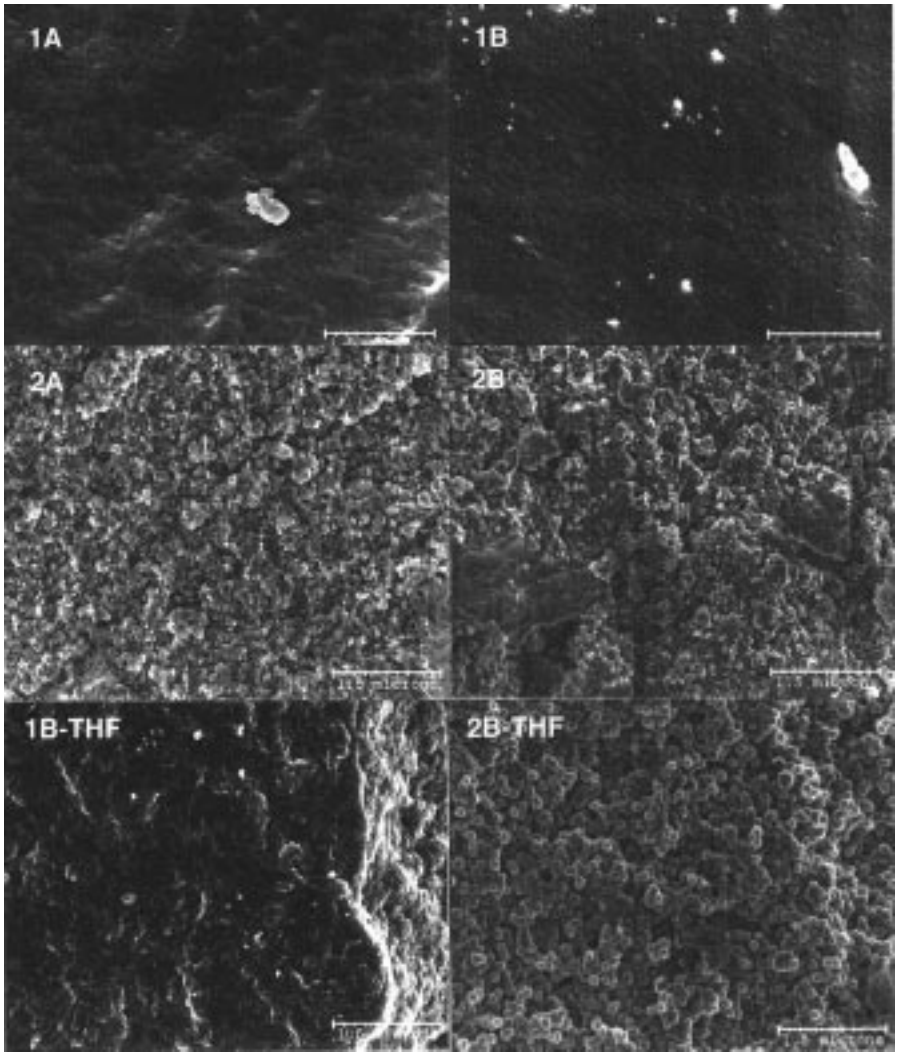

Figure 8. Scanning electron micrographs of xerogels prepared from monomers **1** and **2** under acidic (A) or basic (B) conditions in ethanol or tetrahydrofuran.

the BJH method.[24] A plot of the incremental pore volume vs diameter reveals which pore sizes contribute to the pore volume and to what extent.

The incremental pore volume plots for the ethenylene-bridged polysilsesquioxanes prepared from **1** and **2** under basic conditions are shown in Figure 7. The materials prepared from **1** under basic conditions were found to be almost exclusively microporous (pore diameter < 20 Å) with small contributions to the pore volume from the lower end of the mesopore range (pore diameter 20−50 Å). However, the polymerization of **2** utilizing a basic catalyst yielded materials with very broad distributions of pore sizes. With THF as the solvent, the polymerization of **2** in the presence of NH_3 results in a gradual precipitation of the polymer. This material (**2B-THF**) exhibits significant contributions to the pore volume from both mesoporous (20−500 Å) and macroporous (>500 Å) domains. The maximum contributions to the pore volume in **2B-THF** are from pores with diameters around 290 and 650 Å. When the same polymerization is performed in ethanol, precipitation occurs almost immediately and a material (**2B**) is obtained that shows significant pore volume throughout the mesopore regime with a spike occurring from pores with diameters around 90 Å. The incremental pore volume plots account for the larger average pore diameters observed in **2B** and **2B-THF**. The differences in porosity are attributed to the *E* and *Z* geometries of **1** and **2** since the materials are prepared using identical conditions. The cyclization phenomena observed in **2** may play a role in the formation of the meso- and macroporous domains, possibly by forming macromolecular structures that have a greater disposition toward precipitation. Monomer **3**, which also undergoes cyclization reactions, forms a material (**3B**) with extensive mesoporosity (50−200 Å) under basic conditions and a larger average pore diameter than the xerogels prepared from **1**. The polymerizations of **1** and **2** under acidic conditions result in xerogels that are almost exclusively microporous.

Scanning Electron Microscopy. To provide some insight into the origin of the meso- and macroporosity in materials **2B**, **2B-THF**, and **3B** the polymers were examined by scanning electron microscopy. The electron micrographs shown in Figure 8 show distinctly different morphologies for the polymers prepared from **1** and **2**. Xerogel **1B** exhibits a very smooth morphology with very fine features consistent with the microporous structure identified in the porosimetry studies. How-

(24) Barrett, E. P.; Joyner, L.; Halenda, P. P. *J. Am. Chem. Soc.* **1951**, *73*, 373.

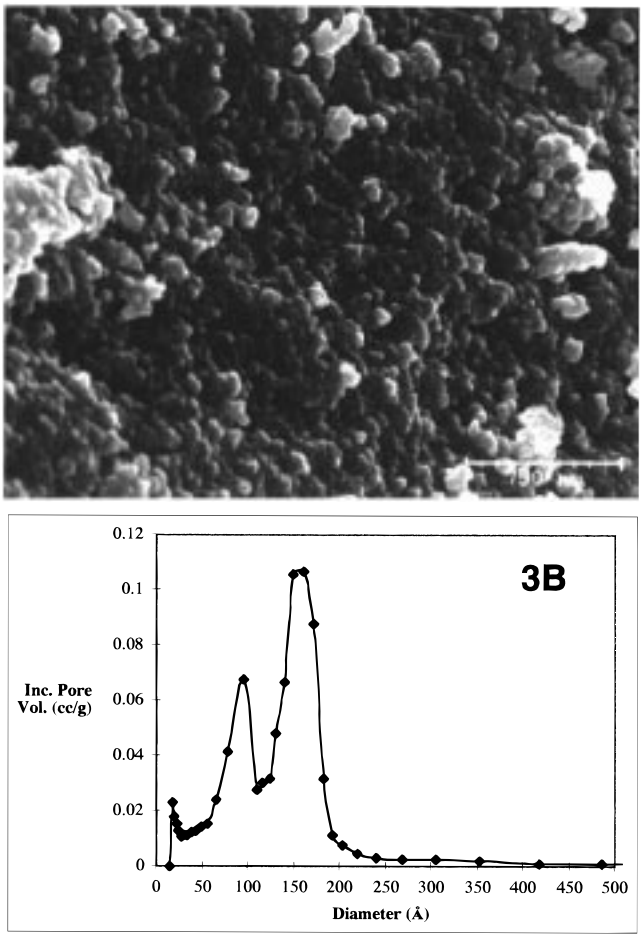

Figure 9. Scanning electron micrograph and incremental pore volume plot of vinylidene-bridged polysilsesquioxane xerogel **3B**.

ever, **2B** has a very rough surface composed of globular structures and fused particulates with diameters of approximately 50−150 nm. The materials prepared in THF show a similar pattern. **1B-THF** has an irregular continuous surface with no distinguishable particulates or globules while **2B-THF** is an aggregate of very uniform spherical particles about 150 nm in diameter. The voids between the particles and globules which make up xerogels **2B** and **2B-THF** are most certainly the source of the meso- and macroporosity observed in these materials.

Monomers **2** and **3**, which have a propensity to form cyclic structures, yield polymers with extensive mesoporous domains. Xerogel **3B** was found to have mesoporosity similar to that of the base-catalyzed materials prepared from **2**, as shown in the incremental pore volume plot in Figure 9. The porosity in this polymer however is limited to pores with diameters smaller than 200 Å. The morphology of this gel is also similar to that of **2B** and **2B-THF** in that the xerogel is an aggregate of spherical particles roughly 50−100 nm in diameter (Figure 9). Although the porosimetry studies did not reveal any profound differences between the gels of **1** and **2** prepared under acidic conditions, SEM studies revealed significantly different morphologies similar to those observed in the base-catalyzed materials. Both **1A** and **1A-THF** have continuous textures with no well-defined particulates (Figure 8). **2A** and **2A-THF** are characterized by rough particulate or globular structures that are much finer (<50 nm in diameter) than those produced from **2** under basic conditions. The formation of mesoporous or macroporous domains in **2A** and **2A-THF** is precluded by the smaller particulates from which the xerogels are comprised.

Conclusions

The orientation of the triethoxysilyl groups in bis(triethoxysilyl)ethenes has a pronounced effect on the hydrolysis and condensation of these monomers and on the materials derived from their polymerization. The formation of a cyclic dimer severely inhibits the polymerization of 1,1-bis(triethoxysilyl)ethene. However, both (*Z*)- and (*E*)-1,2-bis(triethoxysilyl)ethene are readily polymerized under basic or acidic sol−gel conditions to highly condensed xerogels. The polymerization of the *Z* monomer proceeds through cyclic condensation reactions leading to the formation of seven-membered rings from which the network polymer is constructed. No evidence of cyclic condensation products is found during the polymerization of the *E* monomer.

The different polymerization processes for the *Z* and *E* isomers leads to materials with vastly different morphologies and porosities. (*E*)-1,2-Bis(triethoxysilyl)ethene (**1**) yields polymers under acidic and basic conditions that have smooth continuous structures and that are almost exclusively microporous. Materials prepared from (*Z*)-1,2-bis(triethoxysilyl)ethene (**2**) using aqueous HCl as the catalyst are characterized by fine globular structures which are also microporous. However, base-catalyzed polymers derived from **2** are well-defined particulate xerogels when THF is the solvent and fused particulate or globular structures when synthesized in ethanol. These materials exhibit extensive mesoporous and macroporous domains. Since the polymerizations of the cis and trans monomers are conducted under identical conditions, the differences in the ethenylene-bridged polysilsesquioxanes derived from them must arise from the geometrical differences of the silsesquioxane groups about the bridging ethylene group.

Acknowledgment. Sandia is a multiprogram laboratory operated by Sandia Corporation, a Lockheed Martin Co., for the United States Department of Energy under Contract DE-AC04-94AL85000.

CM9805424